

Final
10/1/98
345407

**Final Report for Sounding Rocket Grant NAG5-653
from NASA to the University of Michigan**

John T. Clarke, Principal Investigator

Period of performance: 1 January 1989 - 31 May 1998

This final report reports the activity on this grant through 31 May 1998, after which a new grant to continue this project was put into place. Overall, this project has resulted in 4 launches from the White Sands Missile Range of our payload in different stages of development, on:

4 May 1991	Flight 36.062
16 June 1993	Flight 36.101
1 April 1995	Flight 36.104
28 October 1996	Flight 36.149

For each flight, the following activities were accomplished:

- prepare the experiment, including replacement and upgrading of critical components, at the University of Michigan
- integrate the payload either at the Wallops Flight Facility
- perform final far-UV calibration of instrument
- perform final alignment, integration, and electrical checks at WSMR
- launch payload from WSMR
- check condition of recovered payload
- perform post-flight calibration, if necessary and applicable
- reduce and analyze flight data.

On the following pages, a description of the instrument is presented, along with overviews of the results of the four flights. We are presently preparing the payload for the next flight in 1998/99.

The Sounding Rocket Telescope and Imaging Echelle Spectrograph: The Jupiter Telescope is a Cassegrain design that was originally developed at Johns Hopkins University for use with a sounding rocket payload. The telescope employs a Dall-Kirkham figure for low cost, with a 35 cm diameter ellipsoidal primary and a spherical secondary mirror providing 1-2 arcsec image quality within a few arc min of the optic axis. The telescope delivers a $f/21$ beam to the focal plane with a plate scale of 26 arc sec/mm - the telescope mirrors were re-polished before our second flight above to increase the magnification at the focal plane, and to achieve 1 arc sec image quality. Primary targeting for the Jupiter Telescope is provided by a NASA supplied Ball Aerospace Strap V star tracker. The tracker is co-aligned with the Jupiter Telescope to a post-vibration tolerance of 1 arc min, and has a correction bandwidth of 15 arc sec in pitch and yaw. More precise centering and image motion compensation are achieved by re-imaging a portion of the incoming beam onto a visible sensitive 4-quadrant photodiode star tracker (manufactured by SPACOM Inc.). The SPACOM tracker drives two micrometer servomotors mounted behind the secondary mirror to reposition the secondary mirror in pitch and yaw until the light is equal in all four quadrants. In the most recent flight of the Jupiter Telescope, 1-2 arc sec pointing accuracy and stability was achieved using this compensation scheme, which when convolved with a telescope image of 1-2 arc sec gives a total point spread function of 2-3 arc sec.

The spectrograph has been designed and constructed at Michigan for UV echelle line profile measurements with long-slit imaging. The Ebert-Fastie configuration employed in the design of the spectrograph has many characteristics well suited to the science needs of this mission. Symmetric off-axis reflections from a single collimating mirror are employed to remove aberrations: the spatial resolution is limited by the telescope and the spectral resolution by the grating and aperture characteristics. Use of a paraboloidal collimator, while more expensive than the usual spherical mirror, has produced better than 2 arc sec image quality with minimal astigmatism along the central 2-3 arc min. The Ebert-Fastie configuration has the additional advantage of being relatively insensitive to the incident angle of the incoming beam: near parallel to the optic axis, the spectrograph focuses an image of the aperture at the same location on the detector. This feature greatly facilitates the alignment process and renders the spectrograph insensitive to small movements of the collimating mirror that may occur during launch. A 20° magnesium fluoride (MgF_2) objective prism mounted 48 cm forward of the aperture plate is used to disperse the converging beam from the telescope: with the 1216 \AA image focused onto the primary aperture, other wavelengths are excluded from the spectrograph producing a very low level of scattered light on the detector. The reflected image may also be used to align the telescope with the NASA and SPACOM tracking systems. The entrance aperture plate is milled stainless steel with an optical quality front surface, containing a central and offset sky apertures each 5 arc sec wide and longer than the detector field of view. The spectrograph uses a replica of the STIS E-1 echelle grating manufactured by Hyperfine Optics. The E-1 replica has a 700° blaze and is optimized to the 221st order of 1216 \AA with a groove spacing of $14.5 \mu\text{m}$. For a 5 arc sec aperture width, $R = 3 \times 10^4$ with a theoretical resolution at $\text{Ly } \alpha$ of 0.04 \AA (the achieved resolution of the detector gave 0.055 \AA resolution in the last flight). The interior surfaces of the housing have been glass beaded to reduce reflectivity to stray light. Both the entrance and exit ports as well as the grating are fitted with baffles to trap zero order light and reduce scattered light contamination. The spectrograph can be aligned in air using $\text{H}\beta$ 4862 \AA emission from a hydrogen discharge lamp, which is exactly 4 times the wavelength of $\text{Ly } \alpha$ 1215.67 \AA , saving a great deal of time on alignment in vacuum.

The Microchannel Plate Detectors: High resolution microchannel plate (MCP) imagers with a wedge and strip positioning anode and associated electronics were designed and constructed for this experiment by O. Seigmund at the U. of California Berkeley (UCB). This detector is very similar to those used on the successful EUVE mission as well as a number of other rocket flights. The detector uses four MCPs mounted in a back to back configuration to provide image intensification with a gain of 1.2×10^7 e⁻/photon. A 10,000 Å KBr photocathode was deposited on the upper plate. Measurements with a pin hole mask at the surface of the plates show a resolved pixel of 50 μm or 1.3 arc sec at the plate scale of the Jupiter Telescope. This provides 2 pixels per 2.6 arc sec resolved point at the telescope focus. The spectrum is well sampled by the MCP detector, with 0.011 Å/pixel. The detector readout uses a three electrode wedge and strip anode 2 cm in diameter. The wedge and strip electrodes employ a linearly variable surface area to provide 2-dimensional positioning to a high degree of accuracy with a minimum of geometric distortion. The detector is housed in an evacuated stainless steel housing, and light enters the housing through a 3.8 cm diameter MgF₂ window mounted in a ConFlat flange attached to the front face of the housing. Vacuum is maintained by employing in tandem a 2 liter/sec vacion pump and a passive SAES getter pump. The vacion pump power is supplied externally and so it is deactivated at launch.

Real time display of the detector output is provided by a laptop computer outfitted with a 16 bit parallel port to read in telemetry decommutated by the NASA processing station. These data are converted to positional X,Y values, binned into a screen image, and stored for future playback. This same system is used for laboratory measurements with the detector. Analog data from the charge-amplified wedge, strip, and zigzag anodes of the MCP detector are digitized into three 16 bit values per photon by an analog to digital converter (ADC). The telemetry interface (TM) deck receives all three 16 bit values in parallel from the ADC. The values are latched and then stored in 3 redundant First In First Out (FIFO) memories. The FIFO's are 8 Kbytes deep, so they can store 1365 events at 6 bytes per event. The FIFO's allow data input and output to occur independently so that the pulse pair resolution of the system is limited mainly by the ADC conversion time, which is roughly 10 μsec. Two FIFO outputs are directed to 2 redundant telemetry channels, and each channel can presently transmit 2500 events/sec which is ten times the expected total count rate while observing Jupiter. The third FIFO output is sent to an onboard PC that stores data in battery-powered RAM as a backup in the event of a telemetry failure. Telemetry data are collected using a NASA supplied TD-Plus to extract the MCP data from the telemetry signal and send it to a ground-based PC, which simultaneously stores data to disk and displays it on the screen to allow real time monitoring of data during flight. Final data reduction and analysis are performed on Sun workstations using IDL: analysis procedures exist for the display of rocket data in MCP image and pulse height formats, as well as for the reduction of the echelle spectra.

The Re-Imaging Camera: We have designed and built a camera to re-image the focal plane onto a separate detector, providing an image of the telescope field of view minus the light which passes through the spectrograph apertures. The image on the aperture plate is sufficiently dispersed by the objective prism that the Ly α image of Jupiter's disk is clearly separated from longer wavelength continuum emissions and the bright polar auroral H₂ Lyman bands. The aperture plate is optical quality stainless steel with a Al/MgF₂ coating to reflect the UV light, and the re-imaging optics are an Ebert-Fastie arrangement with a flat mirror in place of the grating. The

image scale at the second detector is the same as at the focal plane, and laboratory tests with a resolution pattern have shown that this system re-images the focal plane with better than 1 arc sec image quality: in this case the overall system resolution is determined by the image quality and target jitter at the focal plane, which is 2-3 arc sec. In earlier flights through April 1995 we used a prototype WFPC 2 CCD for the second detector with a Na Wood's filter at the camera entrance to block the visible light. Now that the WFPC 2 technology has been tested and demonstrated on the HST, we have replaced the CCD with a MCP detector with a KBr photocathode. The main advantage of the MCP detectors is the higher UV quantum efficiency, which is not matched by existing CCD and filter properties. Conservatively assuming 50 μm resolution on the MCP detector, this will provide 1.3 arc sec resolution on the detector or roughly half the resolution of the telescope image, and the image will be well sampled with a pixel size not greater than 0.5 arc sec. The sensitivity of this camera at Ly α is 0.15 cts/sec-kR for a 2.5 arc sec source region, providing a limiting detection of 0.2 kR over a 300 sec rocket integration. The sensitivity will be 50 % higher at 1600 \AA for the auroral H₂ Lyman bands.

The imager is particularly important scientifically because no high sensitivity spectrally pure Ly α image of Jupiter has been obtained since the Voyager epoch in 1979, when the bulge was first detected by this same rocket telescope but at 6 arc sec resolution (Clarke et al. 1980). Testing present theories of the process giving rise to the bulge emission will require a higher angular resolution image, in addition to the line profile spectra. We are particularly interested in imaging the limb brightening of the bulge Ly α emission, as expected from enhanced scattering in the optically thin wings of the line. It has also been suggested that the bulge may be produced by a process analogous to the equatorial anomaly on the Earth, in which case the bulge emission might have a form similar to the tropical arcs observed on the Earth with separate bands at ± 150 magnetic latitude. Similar bands on Jupiter would be separated by roughly 10 arc sec, and the imager is designed to easily resolve such features if they exist in the Ly α bulge on Jupiter. In the next flight to observe Jupiter, we will initially place the aperture north/south across the disk: with the northern auroral hot spot at $\lambda_{\text{III}} = 1800$ near the central meridian, the Ly α bulge will be visible near the receding limb. Although much of the auroral emission will enter the spectrograph aperture, part of the auroral oval and the bulge will be visible to the imager. In the second half of the flight, the aperture will be aligned east/west across Jupiter's disk, and both north and south auroral zones will be imaged for a real-time measurement of the auroral pattern that has passed through the spectrograph aperture during the north/south alignment. The imager will also provide a direct measurement of the positioning of the aperture on Jupiter during each integration.

Calibration Data and Previous Flights: The throughput of the instrument has been determined in addition to overall system measurements by successive placement of each optical component in a vacuum chamber (the CTE) at Johns Hopkins U. (JHU), and by measuring the transmission with a calibrated photomultiplier. The detector quantum efficiency (QE) was determined by comparing the count rate signal with a direct measurement onto the photomultiplier.

The total sensitivity of the instrument in counts/sec - Rayleigh may be expressed as:

$$S_{\lambda} = \{ [10^6/4\pi] A_j Q_j A_s Q_{\text{LiF}} Q_{\text{MCP}} Q_{\text{Coll}}^2 G_{\text{eff}} \} * DT$$

where A_j = area of the Jupiter Telescope primary (cm^2), Q_j = measured throughput of the Jupiter Telescope, A_s = area of the entrance aperture (steradians), Q_{LiF} = transmission of the predisperser,

Q_{MCP} = efficiency of the detector and MgF_2 window, Q_{Coll} = reflectivity of the parabolic mirror, G_{eff} = mean efficiency of the grating into the desired order, and DT = the signal dependent dead time correction. The full detector dark count rate is 1-3 counts/sec. The results of the throughput test yield a combined effective area of 6 cm², or a sensitivity $S_\lambda = 50$ counts/kR in 300 sec (the length of the rocket observation) for a 3 arc sec (along the aperture) by 5 arc sec (the width of the aperture) emission source. Since Jupiter's emission is 10 kR (dayglow) to several hundred kR (aurora), we expect good signal to noise even in the limited duration of one rocket flight. The sensitivity to more diffuse emission is higher by the ratio of aperture areas: for the ISM emission covering 5 arc sec by 6 arc min by three apertures, we achieve 18 counts/Rayleigh in 300 sec. Calibration spectra of a hydrogen and a deuterium lamp were taken to determine the wavelength dispersion of the spectrograph. Both lamps provide a Ly α feature that is broad relative to the theoretical resolution of the spectrograph (spectra of a Pt-Ne lamp are taken to determine the instrument wavelength resolution. H Ly α and D Ly α are clearly separated, and the self absorbed minimum in each line is clearly resolved. The dispersion measured by centering on the two lines is .35 Å/mm, consistent with that obtained from a ray trace using the BEAM4 program.

May 1991 Flight 36.062: The first flight of the payload occurred on 4 May 1991 from the White Sands Missile Range. An apparent yaw crosstalk error associated with the NASA star tracker prevented the acquisition of Jupiter by our telescope. This malfunction appears to be identified with use of the tracker and flight electronics, and is characterized by a change in the yaw position readout that is dependent on the input line voltage. NASA has analyzed this malfunction and the problem appears to be unique to the tracker unit in our 1st flight. Analysis of the magnitude of the yaw error is limited by the 5 arc min field of view of the SPACOM tracker. While no positive detection of a bright object was made by the tracker, a low level of signal was recorded in all four quadrants of the SPACOM photodiode. This may indicate scattered light reflecting off the inner surface of the tracker entrance baffle, which would indicate an error of 5-10 arc min. Preflight alignment of the telescope, SPACOM tracker, and NASA tracker was performed to a post-vibration tolerance of ± 1 arc min. A postflight test of the co-alignment was performed at UM in July of 1991. The NASA tracker, which had been removed from the payload prior to its return shipment from WSMR, was reinstalled, and its alignment compared with preflight measurements. No significant change in the alignment was discovered that could account for the flight error. To avoid this specific problem in future missions, a protocol will be added to the alignment procedure to connect the NASA tracker to its flight electronics and test the alignment at different line voltages. To decrease our sensitivity to misalignment in general, other modifications are proposed (sec. 2.5) for the telescope. Despite the malfunction in the tracking system, the flight did demonstrate the performance characteristics of the instrument. A spectrum of the Earth's geocoronal Ly α emission was obtained, as well as a 5 σ detection of Ly α associated with the interplanetary medium. All optics were protected from reentry by a cover plate, and none were damaged in the flight or landing. Post flight disassembly of the payload revealed no damage to any of the flight components, and the telescope mirrors were well protected by the NASA-supplied aperture door.

Analysis of the geocoronal Ly α emission feature shows a FWHM of .07 Å: the line is not resolved and the profile represents the instrument resolution limit. Grating scattered light contributed a background signal at 15% of the peak at Ly α : this high level was due to 3 overlapping coatings of Al/MgF₂ on the grating, which had been applied in attempts to optimize the

reflective efficiency. Now that we have learned how to optimize the coating on a large 700 grating, a single coating will suffice the next time around and the level of scattered light can be greatly reduced: independent measurements of this grating by the STIS project before coating indicated a groove efficiency of 70% and scattered light wings less than 1 % of the peak (C. Bowers, pers. comm.). The measured counting rate for the flight was 15 events/second (of which less than 1 count/sec are detector dark counts), and a near-simultaneous measurement of the geocoronal emission along a similar line of sight with a JHU airglow instrument gave 2.3 kR at Ly α (P. Feldman, pers. comm.). This value is used to obtain a 1.0 cm² effective area for the telescope / spectrograph combination. Resonantly scattered Ly α from the ISM was resolved as a 5 σ feature separated by approximately .18 Å from the geocoronal line: this bulk Doppler shift is consistent with the known combined Earth orbital and ISM motions along the line of sight. This emission has a brightness of 300 R, and a FWHM of roughly 0.16 Å which is much greater than the instrumental resolution! For the 4 May 1991 launch date, the line of sight toward Jupiter was 50° from the downstream direction. With the .07 Å resolution in the 1st flight, the instrument would not resolve the 8000 K ISM neutral temperature determined from previous observations with a hydrogen absorption cell⁶. The observed broadening may be due to a scattering of particle trajectories in the downstream direction of the flow that is caused by the interaction of the material with the solar gravity. We will model the line profile based on the line of sight velocity components expected from interplanetary hydrogen and compare the results with our own independent observations with the HST/GHRS later in May 1991 toward Mars.

June 1993 Flight 36.101: In this flight we experienced a failure in the telemetry of part of the flight data, including the MCP detector data in the sense that the flight data were received in a garbled state on the ground. Repeated ground tests were unable to reproduce the exact nature of the corrupted data, but we found that we could create a similar corrupted bit pattern by interrupting the synchronization between our detector and the NASA telemetry. The evidence from extensive post-flight testing suggested that the detector performed nominally, but that an intermittent connection had corrupted the telemetry stream. To ensure that this intermittent problem would be corrected, we a) replaced all wiring between our detector and the NASA telemetry encoder, b) introduced an on-board storage buffer in our payload to store the MCP data directly from the detector, and c) introduced redundant data transfer and telemetry to the ground. At this time we also replaced the MCP detector with a new, higher resolution detector and signal processing electronics. In the April 1995 flight, both telemetry channels relayed the MCP data stream without error, and these data were consistent with the data stored in our experiment buffer. We have therefore demonstrated in flight that these earlier problems have been corrected, and a spectrum of the geocoronal and ISM Ly α lines is shown in the figures.

The April 1995 Flight 36.104: In the April 1995 flight, the above mentioned systems functioned nominally but we recorded high voltage discharge or arcing on the MCP detector and a negligible count rate from that detector. Operation of the detector immediately post-flight showed a zero count rate, while after the instrument was returned to Michigan and the skin sections removed the detector again functioned normally. The return to normal operation indicated that the arcing had not been internal to the detector, and subsequent testing in Michigan and by Ossy Seigmund in Berkeley has confirmed this. We initially suspected a breakdown in the high voltage connector at the point where it is attached to the detector. The connector is a Reynolds 600 series connector,

which is necessary due to limited space at the back of the detector. This connector has been in common use on rockets for at least two decades, and they are known to be reliable if properly prepared and tightened down but subject to arcing if improperly prepared and/or attached. The connectors have a vacuum feed-through arrangement with a small insulating O-ring seal, which needs to be carefully cleaned before each use to prevent the build up of metal deposits that can accumulate from the threaded walls of the connector, and the connector must be tightened to the correct pressure to ensure a good seal. Operation of this connector with external pressures in the breakdown range can in principle contribute to arcing across this seal. In post-flight testing, before any disassembly of the detector we first tested the system in the large vacuum chamber at WFF. Three days of vacuum pumping tests at all pressures from atmospheric to 10^{-5} Torr yielded 5 single arcing events, compared with events roughly every 10 sec. in flight. Later disassembly of the connector showed a clear dark brown current discharge path across the insulating O-ring, confirming the proposed phenomenon. Detailed testing at Michigan, Wallops, and Berkeley has shown no other problems with the detector. We interpret the low count rate in flight as due to insufficient voltage across the channel plate stack for photon-counting above the discriminator threshold, and we have found that HV arcing events can cause the signal processing electronics to lock up so that real photon events after the first arcing event would not be recorded.

October 1996 Flight 36.149: To prevent HV arcing as experienced during the previous flight, we performed thorough testing of the MCP detectors before flight, including repeated operation at all external pressures, and after this testing the connectors were not unplugged before flight. We also tested the response of our signal processing electronics to simulated arcing events to develop a system that can recover and continue counting photons even if an event were to occur in the detector high voltage system. In addition, in the October 1996 flight we had two MCP detectors, so that a mission success could be achieved with flight data from either detector, although experience has shown that known problems are *always* corrected and problems that do occur are due to elements that have not received sufficient attention. This had been the first failure due to the experiment in this project, and it was corrected in the October 1996 flight.

Sounding rocket flight 36.149 was launched the night of 28 October 1996 from the White Sands Missile Range, and all of the success criteria were met in this flight. We are now involved in post-flight calibration work and reduction of the flight data. Both the set-up star (Altair) and Jupiter were acquired by the ACS on time, and our payload startracker centered the images of both objects at the correct location on our aperture plate for H Ly alpha emission to enter our aperture. Jupiter was tracked to within 1-2 arc sec, as expected, and both MCP detectors functioned as expected with no high voltage glitches. We clearly see the UV image of Jupiter in the quick-look MCP data, however the count rates on both detectors were lower than we had expected. We are now engaged in post-flight measurements to determine the source of the lower than expected throughput in the instrument, and we will be performing a detailed analysis of the flight data over the months to come in preparation for publication of the data. We have received the payload back in good condition, and we look forward to future flights.

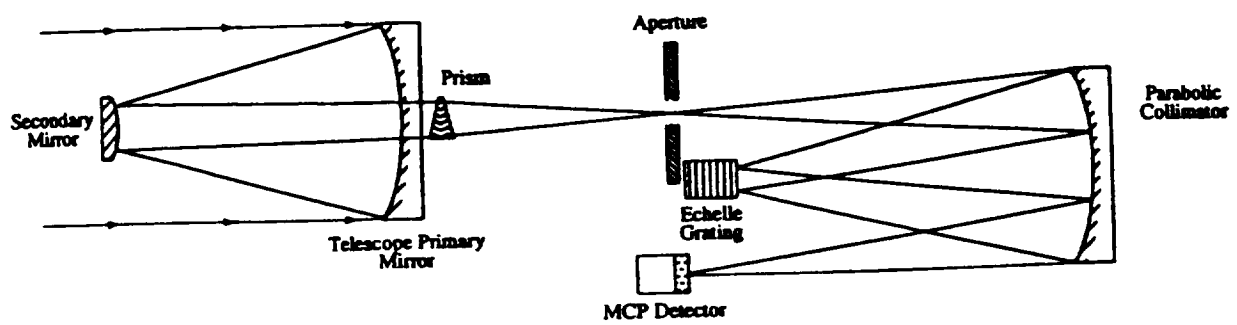


Figure 1. Schematic optical layout of existing Jupiter telescope and echelle spectrograph.

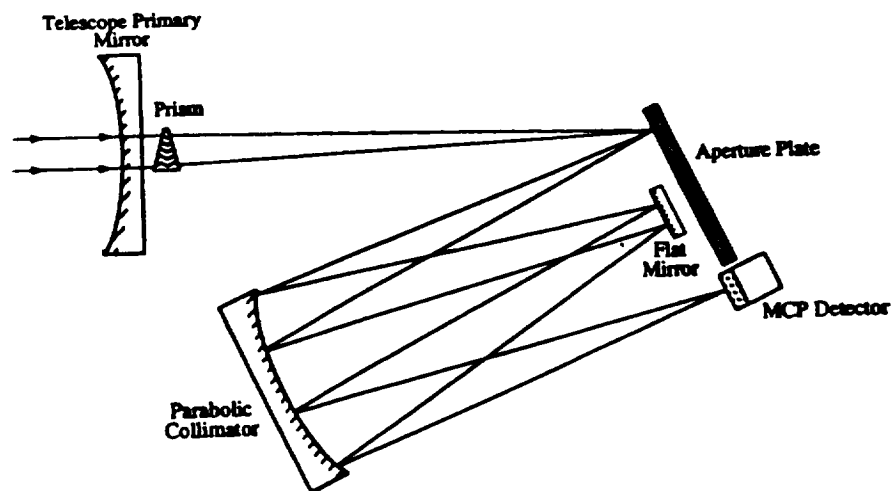


Figure 2. Schematic of existing optics for re-imaging the focal plane onto a separate MCP detector by means of a reflection from the mirrored aperture plate.

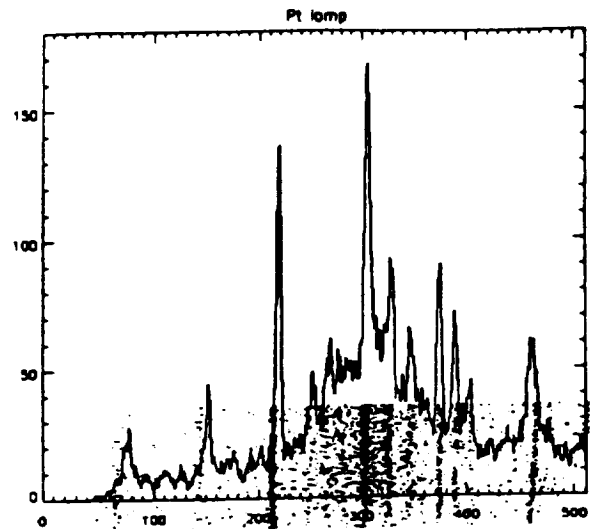
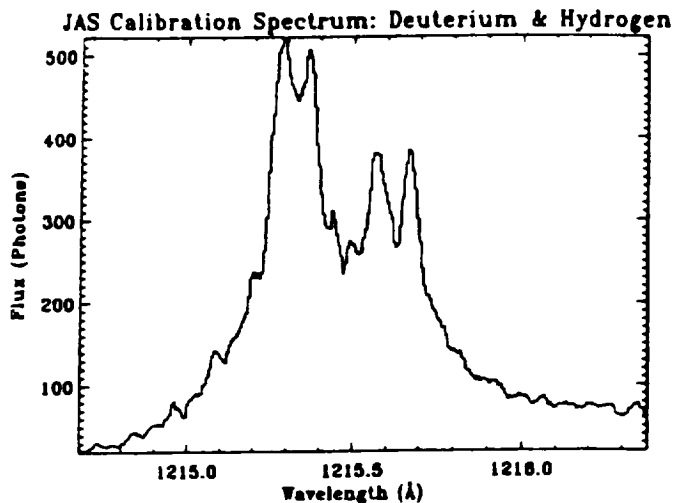


Figure 4. a) Laboratory spectra of D (1215.33 Å) and H(1215.67 Å) Ly α lines from a D₂ lamp, showing the broad self-absorbed character of these lines, and b) lab. spectrum of a Pt-Ne hollow cathode lamp, showing the 0.055 Å resolution of the instrument on a nested series of intrinsically narrow Pt lines: in this figure an image of the spectrum is overlotted with an intensity trace.

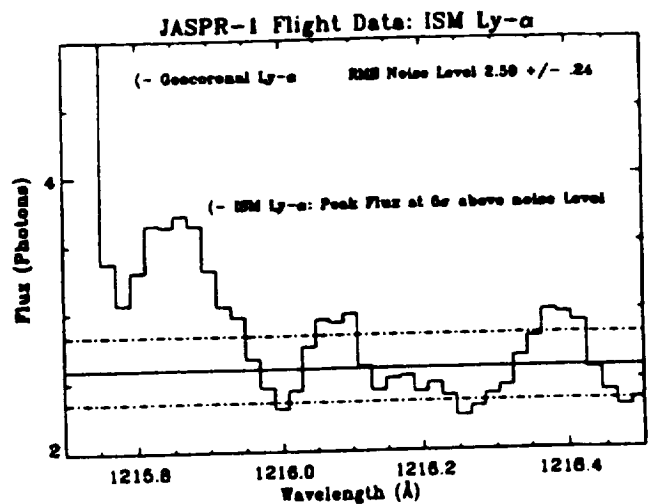
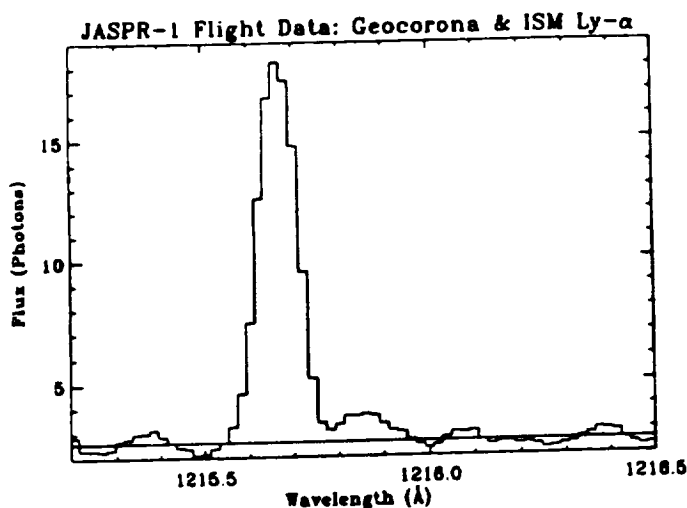


Figure 5. a) Flight spectrum (May 1991) of geocoronal H Ly α line profile, and b) expanded plot of flight spectrum showing resolved ISM H Ly α emission line. The present sensitivity is 20 times greater than this, due to higher efficiency and much larger sky apertures in the system.

Publications Relevant to this Sounding Rocket Program

Instrument:

"A small plane grating monochromator", W.G. Fastie, *Journal of the Optical Society of America*, 42, pp. 641, 647, 1952.

"A rocket telescope spectrometer with high precision pointing control", M. Bottema, W.G. Fastie, and H.W. Moos, *Applied Optics*, 8, No. 9, 1821, 1969.

"Spatial imaging of hydrogen Ly α emission from Jupiter", J.T. Clarke, H.A. Weaver, P.D. Feldman, H.W. Moos, W.G. Fastie, and C.B. Opal, *Astrophys. J.*, 240, 696, 1980.

"High resolution, two-dimensional imaging, microchannel plate detector for use on a sounding rocket experiment", B. Bush, D. Cotton, O.H. Siegmund, S. Chakrabarti, W. Harris, and J.T. Clarke, *Proceedings of the SPIE*, 1549, 290, 1991.

"High Resolution Ultraviolet Spectrograph for Sounding Rocket Measurements of Planetary Emission Line Profiles", W.M. Harris, J.T. Clarke, J.R. Caldwell, P.D. Feldman, B.C. Bush, D.M. Cotton, and S. Chakrabarti, *Optical Engineering*, 32, 3016, 1993.

Science:

"Deuterium Content of the Venus Atmosphere", J.L. Bertaux & J.T. Clarke, *Nature*, 338, 567, 1989.

"HST/GHRS Observations of the Interplanetary Medium Downwind and in the Inner Solar System", J.T. Clarke, R. Lallement, J.L. Bertaux, & E. Quemerais, *Astrophys J.*, 448, 893, 1995.